RSC Advances

ROYAL SOCIETY OF CHEMISTRY

www.rsc.org/advances

Adsorption and recovery of U(VI) from low concentration uranium solution by amidoxime modified *Aspergillus niger*

Le Li[a, b], Nan Hu[a], Dexin Ding[a, *], Xin Xin[a], Yongdong Wang[a], Jinhua Xue[a, b], Hui Zhang[a], Yan Tan[a, b]

[a]Key Discipline Laboratory for National Defense for Biotechnology in Uranium Mining and Hydrometallurgy, University of South China, Hengyang 421001, P. R. China

[b]School of Public Health, University of South China, Hengyang 421001, P. R. China

Le Li and Nan Hu contributed equally to this work

*Corresponding author. Tel.: +86 734 8282534.

E-mail address: dexinding58@126.com (Dexin Ding)

Abstract

The amidoxime modified *Aspergillus niger* (AMAN) was prepared by the oximation reaction. The effects of the initial pH, contact time, initial U(VI) concentration and biosorbent dose on the adsorption of U(VI) ions from radioactive wastewater in U(VI) concentration of less than 1 mg/L by AMAN and the raw *Aspergillus niger* (RAN) were investigated. The maximum adsorption efficiency by AMAN for 0.5 mg/L U(VI) solution amounted to 98.85% under the optimum adsorption conditions, while the maximum adsorption efficiency by RAN was only 77.83%. The adsorption equilibrium data were found to be best fitted to Langmuir isotherm model, and the maximum biosorption capacity of AMAN for U(VI) was estimated to be 621 mg/g at 298 K. The biosorption kinetics followed the pseudo-second order model and intraparticle diffusion equation. The Gibbs free energy change (ΔG^0), enthalpy change (ΔH^0) and entropy change (ΔS^0) showed that the adsorption process of U(VI) was spontaneous, feasible and endothermic. The SEM-EDS study indicated that much more U(VI) ions were adsorbed by AMAN than by RAN. FT-IR study showed that the $-NH_2$ and =N-OH groups of amidoxime were the dominant ones for binding UO_2^{2+} ions. Moreover, AMAN was found to have excellent selective adsorption capability of U(VI) due to amidoxime groups. The UO_2^{2+} ions adsorbed by AMAN

could be desorbed using 0.1 M HCl, and the desorption efficiency reaching 87.28% at the 8th cycle of adsorption and desorption.

Keywords: amidoxime; *Aspergillus niger*; modification; biosorption; uranium

1. Introduction

Uranium mining and processing generate huge amounts of radioactive wastewater with U(VI) concentration of lower than 1.0 mg/L. Once the radioactive wastewater is released to the environment, the surface water and groundwater will be contaminated [1]. U(VI) in the surface water and groundwater, even at low concentration, can be accumulated in aquatic animals and human beings and be harmful to their lung, liver, spleen and marrow [2]. Therefore, the radioactive wastewater has to be treated before being discharged.

But so far, the efficient methods have not been proposed for treating the low concentration radioactive wastewater [3]. Fortunately, many previous studies have been conducted on the feasibility, hydrophilia and selectivity of sobents and could help to prepare the sorbent with good feasibility, hydrophilia and selectivity for adsorption of U(VI) ions from the low concentration radioactive wastewater.

Biosorption has been found to be more feasible than the traditional methods such as precipitation, coagulation, solvent extraction, etc. [4, 5], and some natural biomaterials such as fungi, marine algea, bacteria and

industrial wastes have been found to have potential towards treating toxic heavy metals [6, 7]. Although these materials in their natural state have low biosorption capacity for the U(VI) ions in radioactive wastewater [8], their adsorption performance can be improved by esterification, graft copolymerization and crosslink, and their adsorption capability can be increased by chemical surface modifications such as acid and organic solvent modifications [9-11]. Especially, *Aspergillus niger* has been found to have good hydrophilia and many active groups for U(VI) ions such as carboxyl and phosphate on its surface [12].

In addition, various functional groups have been studied for uranium recovery from low concentration radioactive wastewater. Among them, the amidoxime has been found to have both acidic oxime and basic amino groups, and its prominent selective adsorption behavior has been found to depend on the lone pairs of electrons in oxime oxygen and amino nitrogen which can be donated to the positive metal center to form a stable five-membered chelate with U(VI) [13-14]. Consequently, the amidoxime group has been used to functionalize various adsorbent substrate materials, and the amidoxime functionalization has been found to improve the sorption capacity and selectivity for U(VI) ions from the low concentration radioactive wastewater. But it can hardly be used for actual wastewater remediation due to its weak hydrophilia.

Therefore, if *Aspergillus Niger* is functionalized by amidoxime, it

should possess the advantages of the two materials, and it would be a promising effective and economical candidate for adsorbing and recovering U(VI) from radioactive wastewater with U(VI) concentration of lower than 1 mg/L. In the present work, the amidoxime-modified *Aspergillus niger* (AMAN) was prepared, its selective adsorption capacity and desorption efficiency were studied, the effects of initial pH, contact time, initial U(VI) concentration and the biomass dose on its biosorption of U(VI) were investigated, the mechanism for removing U(VI) from low concentration radioactive wastewater by the AMAN was analyzed, and the experimental data were fitted using different models and the process parameters were evaluated. Based on the experimental results, the application possibility of AMAN for the adsorption and recovery of U(VI) from low concentration uranium-bearing aqueous solutions was evaluated.

2. Materials and methods

2.1 Preparation of RAN

The *Aspergillus niger* biomass, was isolated from uranium wastewater and identified by microbial type culture collection (MTCC), Guangdong Institute of Microbiology, China. The biomass was cultured in potato-dextrose agar (PDA) liquid medium containing potato (200 g), sucrose (20 g), and distilled water (1 L). The inoculated medium with optical density (OD) of 0.1 was cultured on a rotary shaker at 298 K and

200 rpm for 2-3 days. The myceliums of *Aspergillus niger* were obtained by filtrating the culture fluid with gauze and rinsed with distilled water until the filtrate was neutralized. The biomass was then grinded after it was dried at 323 K for 24 h and was sieved through 100 mesh sieve. The resulted biomass was referred to as the raw *Aspergillus niger* (RAN).

2.2 Preparation of AMAN

As shown in Fig.1, AMAN was prepared in the following three steps.

(1) Modifing RAN with silane coupling agent KH-570: 6 g of the dried RAN sample was immersed in 120 mL of absolute ethanol, together with 6.5 mL of deionized water, 4 mL of 25 wt% aqueous ammonia and 2 mL of a silane coupling agent KH-570. The mixture was then continuously stirred at 328 K for 48 h. The precipitate was washed repeatedly with absolute ethyl alcohol so as to remove the remaining KH-570 and was then dried in a vacuum oven to the constant weight.

(2) Grafting acrylonitrile (AN) onto the KH-570 modified RAN: 1.23 g of KH-570 modified RAN, 100 mL of N, N-dimethyl formamide (DMF) solution containing 11.79 mL of AN, and 0.143 g of azodiisobutyronitrile were added into a four-necked, round-bottomed flask equipped with electric mixer, reflux condenser pipe and thermometer. The graft polymerization reaction lasted for 5 h in N_2 atmosphere at a constant temperature of 348 K.

(3) Oximation reaction: 0.7607 g of NH_2OH•HCl crystal was dissolved

with 22.0 mL of distilled water in a three-necked flask, 0.5801 g of Na_2CO_3 was then added into the solution through stirring it in a N_2 atmosphere. 1 g of powders obtained from step (2) was added into the flask at 343 K, and the mixture was stirred for 4 h until the Na_2CO_3 was completely dissolved [15]. After that, the solution was filtered and washed with deionized water to the neutral. The product was dried in a vacuum oven at 323 K to obtain the AMAN.

2.3 Reagents

Sodium carbonate, hydroxylamine hydrochloride ($NH_2OH{\cdot}HCl$), N, N-dimethyl formamide (DMF) were purchased from Tianjin Kermel chemical reagents development center. The KH-570 and PAN were purchased from Zibo Xin Luyuan bio-chemical Co., Ltd. All the reagents used were of analytical grade without further purification. Ultrapure water (resistivity of 18 $M\Omega\ cm^{-1}$) used in the experiments were produced by the Central Distilled Water System Platform (CN120RDM1-230). The standard stock solution of uranium (1 g/L) was prepared by dissolving 1.1792 g U_3O_8 with 10 mL of hydrochloric acid, 3 mL of hydrogen peroxide and two drops of nitric acid, and the mixture was then heated by a sand bath. The test solutions of U(VI) were prepared by diluting the stock solution of U(VI) to the desired concentrations, and finally negligible amount of 0.1 or 0.01M HCl or NaOH was added to adjust the initial pH values of the test solutions.

2.4 Instrumentation

The trace uranium analyzer (WGJ-III, China) was used to measure the concentration of uranium in solutions. The precision pH meter (PB-20(PB-S), Germany) calibrated by the buffer solutions (pH 4 and 6.86) was used to adjust the pH of the solutions. The liquid medium was autoclaved at 394 K for 20 min in an autoclave (VB-40, Germany). The plates used for cultivating *Aspergillus niger* were placed in the water-jacket thermostatic constant incubator (GSP-9080MBE, China). The modified biomass was dried by the vacuum drying oven (BZF-50, China). The Central Distilled Water System Platform (CN120RDM1-230, UK) was used to provide distilled water for the batch biosorption experiments.

2.5 Batch biosorption experiments

Biosorption experiments of U(VI) by the RAN and the AMAN were conducted in conical flasks (150 mL) to compare their biosorption capabilities. Unless otherwise stated, 0.02 g RAN and AMAN were added to 100 mL of 0.5 mg/L U(VI) solutions, respectively, and the mixtures were then shaken on a rotary shaker at 200 rpm and 298 K for 3 h. After that, 2 mL of the mixture was centrifuged at 8000 rpm for 5 min, and 1 mL of the supernatant was used to analyze the residual concentration of U(VI) by WGJ-III type trace uranium analyzer.

The influence of pH, contact time and biosorbent dose was investigated

in the bach experiments. All the experiments were performed in triplicate, and the data were analyzed by origin software (Version 8.0, USA).

The adsorption capacity of the adsorbent q (mg/g), the removal efficiency $R\%$ and the adsorption distribution constant K_d (mL/g) were calculated from Eq (1), Eq (2) and Eq (3), respectively [16]:

$$q=\frac{(c_0-c_e)\ v}{m} \quad (1)$$

$$Removal\ percent\ (\%)=\frac{(C_0-C_e)}{C_0}\times 100 \quad (2)$$

$$K_d=\frac{(C_0-C_e)}{C_e}\times\frac{V}{m} \quad (3)$$

where C_0 and C_e are the initial and equilibrium concentrations (mg/g) of UO_2^{2+}, respectively, V and m are the volume of uranium solution (L) and the mass of the adsorbent (g), respectively, and K_d is the equilibrium distribution coefficient that represents distribution of the adsorbate in the solid phase and liquid phase.

3. Equilibrium and kinetics studies

3.1 Equilibrium isotherm models

The biosorption equilibrium data were modeled by the Langmuir, Freundlich and the Dubinin-Radushkevich (D-R) models.

The Langmuir isotherm can be expressed as Eq (4) [17, 18]:

$$\frac{1}{q_e}=\frac{1}{q_{max}}+(\frac{1}{bq_{max}})\frac{1}{c_e} \quad (4)$$

where q_e is the biosorption capacity of the biosorbent at equilibrium

(mg/g), q_{max} is the maximum amount of the adsorbed uranium (mg/g), C_e is the concentration of uranium at equilibrium (mg/L), and b is the Langmuir constant (L/mg).

The important characteristics of the Langmuir isotherm can be described by a dimensionless parameter R_L, which is referred to as the separation factor or equilibrium parameter and is defined by the following equation [19]:

$$R_L=\frac{1}{1+bC_0} \quad (5)$$

R_L can indicate whether the adsorption process is irreversible, or favorable, or linear, or unfavorable, in terms of $R_L = 0$, or $0< R_L < 1$, or $R_L =1$, or $R_L >1$.

The Freundlich isotherm can be expressed as follows [20]:

$$lnq_e=lnK_F+\frac{1}{n}lnC_e \quad (6)$$

where K_F and n are the Freundlich constants and adsorption intensity, respectively.

The D-R isotherm can be expressed as follows [19]:

$$lnq_e=lnq_m-\beta\varepsilon^2 \quad (7)$$

where q_m represents the theoretical biosorption saturation capacity (mol/g), β is the activity coefficient related to the mean energy of biosorption (mol^2/J^2), and ε is the Polanyi potential ($\varepsilon=RTLn(1+\frac{1}{C_e})$).

The free energy E (kJ/mol) for the adsorption is calculated as follows:

$$E=\frac{1}{\sqrt{-2\beta}} \quad (8)$$

The biosorption process is of ion-exchange when E is between 8 and 16 kJ/mol, and is of physical when E is smaller than 8 kJ/mol [21].

3.2 Kinetic studies

The experimental data can be modeled by using the Lagergren first-order, Ho's second-order and intraparticle diffusion models. They are presented as follows [22-24]:

The linear form of the Lagergren pseudo-first order kinetic equation is given bellow:

$$log(q_{e1}\text{-}q_t)=logq_e-\frac{k_1}{2.303}t \quad (9)$$

The linear form of the pseudo-second order kinetic equation is expressed as:

$$\frac{t}{q_t}=\frac{1}{K_2q_e^{\,2}}+\frac{t}{q_e} \quad (10)$$

The initial sorption rate equation is as follows:

$$h=K_2q_e^{\,2} \quad (11)$$

The intraparticle diffusion equation is described as:

$$q_t=K_{id}t^{\frac{1}{2}} \quad (12)$$

where q_t is the amount of U(VI) adsorbed at time t (mg/g), q_e is the theoretical value of U(VI) equilibrium adsorption onto the adsorbent (mg/g), q_{e1} is the experimental equilibrium quantity (mg/g), K_1 and

K_2 are the rate constants for pseudo first order (min^{-1}) and pseudo second order kinetic models (g/mg/min), respectively, and K_{id} is the rate constant for intraparticle diffusion model (g/mg/min).

3.3 Thermodynamic studies

The thermodynamic parameters including the standard Gibbs free energy change (ΔGº), standard enthalpy change (ΔHº) and standard entropy change (ΔSº) are the basic indicators for determining whether the adsorption reaction of U(VI) is spontaneous and whether the adsorption reaction is endothermic or exothermic one [25,26].

The value of ΔGº can be calculated from the following equation:

$$\Delta G^0 = -RTlnK_d \quad (13)$$

The relationship between ΔS^o and ΔH^o can be presented as follows [27]:

$$lnK_d = \frac{\Delta S^0}{R} - \frac{\Delta H^0}{RT} \quad (14)$$

where K_d, T and R denote the adsorption distribution constant, the absolute temperature (K) and the gas constant ($R = 8.314 \times 10^{-3} KJ/mol.K$), respectively.

3.4 Characterization

The changes in chemical structure of the biosorbents were characterized by Fourier transform infrared spectrometer (IR Prestige-21, Japan). The variations of the surface morphology of RAN and AMAN were observed using the scanning electron microscopy (JSM-6360LV, Japan). The element types of the AMAN after the adsorption treatment

were analyzed using the energy disperse spectroscopy (EDX-GENESIS60S, Germany).

3.5 The elution of U(VI) and regeneration of the biosorbent

Desorption solutions including HCl, HNO_3, NaOH, Na_2CO_3, $NaHCO_3$ and EDTA-NA were used to release the U(VI) adsorbed on the AMAN. The AMAN sample was mixed with 50 mL regenerating solution with the concentration of 0.1 mol/L and kept shaking in a rotary shaker at 298 K and 200 rpm for 3 h. Then, the AMAN was washed repeatedly with distilled water until the pH of the desorption solution became neutral. After the best desorption solution was selected, the adsorption-desorption was cycled 5 times to observe the regeneration performance of the AMAN. The desorption percentage (%) was presented as follows [28]:

$$Desorption\ (\%) = \frac{the\ \ amount\ \ of\ \ desorbed\ \ U(VI)}{the\ \ amount\ \ of\ \ biosorbed\ \ U(VI)} \times 100\% \quad (15)$$

4. Results and discussion

4.1. Material characterization

4.1.1 FT-IR

Fig.2 shows the FT-IR spectra for RAN and the AMAN before and after adsorption treatment. Curve (a) exhibited the O-H stretching and bending bands at 3381 cm^{-1} and 1641 cm^{-1}, respectively. In addition, the adsorption bands at 2926 cm^{-1} and 1026 cm^{-1} belonged to C-H stretching and bending modes, respectively [29]. Curve (b) showed that the peak at 3381 cm^{-1} decreased significantly and shifted to 3419 cm^{-1}, and this was

probably due to the modification with KH-570. A new peak was observed at 2243 cm^{-1} in curve (c), indicating that nitrile functional groups were grafted on the surface of KH-570 modified *Aspergillus Niger* [30]. However, it was disappeared in curve (d), and two new bands of C=N and N–O appeared at 1577 cm^{-1} and 920 cm^{-1} [31], which demonstrated that interaction between PAN-*Aspergillus Niger* and hydroxylamine hydrochloride ($NH_2OH \cdot HCl$) took place on the surface of the biomass. Curve (d) showed the FT-IR spectra of the PAN-*Aspergillus Niger* after adsorption of U(VI). It could be seen from Fig.1 that the peak at 1577 cm^{-1} in curve (d) shifted to 1550 cm^{-1} in curve (e), and this indicated that the amidoxime groups were involved in uranium uptake [31]. It could be found by comparing curve (a) with curve (d) that the board peak at 3381 cm^{-1} shifted to 3394 cm^{-1}, and this indicates that the $-NH_2$ and =N-OH groups of amidoxime could interact with U(VI) through electrostatic interactions and hydrogen bonds [32].

4.1.2 SEM

The microstructures of RAN, AMAN before and after adsorption of U(VI) were characterized by SEM, as shown in Fig.3. RAN had a rough surface structure in Fig.3(a), and this indicates that the diameter of RAN was about 10~20 μm. Fig.3(b) shows that the average size of AMAN was larger than RAN, and its crumpled, loose and porous surface structure suggests that *Aspergillus Niger* was modified by the amidoxime.

Furthermore, the surface of the AMAN after adsorption of U(VI) became denser, flatter and smoother, as shown in Fig.3(c), which may be attributed to the associated adsorption effects of the -NH2 and =N-OH groups. SEM, FT-IR and EDS characterizations show that the amidoxime groups complexed with U(VI) ions.

4.1.3 EDS

The SEM-EDX images of AMAN after adsorption of U(VI) were shown in Fig.4. A little powder that was dried in vacuum at 298 K for 24 h was placed on a cover slip, transferred to a stub and sputter-coated with 4 nm of gold particles [16]. It can be seen from the analysis of the elemental composition of the sample showed in Fig.4(b) that the U(VI) adsorbed on the AMAN amounted to 6.16%. This indicates that the AMAN could adsorb U(VI) efficiently. The existence of Au, which accounted for 60.64%, was due to the fact that the sample surface was coated with gold for improving surface conductive performance [16, 28].

4.2 Effect of initial pH

The effect of pH on U(VI) adsorption on RAN and AMAN was investigated at sodium carbonate-bicarbonate buffer system. As shown in Fig.5, the adsorption efficiency of U(VI) by AMAN increases with pH when it varies from 2.0 to 5.0, and then decreases with pH from 5.0 to 10.0. The maximum adsorption efficiency of U(VI) by AMAN was 98.85% at pH 5, far more than 77.83% by RAN at pH 7. The results

indicate that the AMAN has great potential for removal of U(VI)，and that pH values influence both the relative distribution of U(VI) species in solutions and the surface properties of AMAN. From the relative distribution of U(VI) species in solutions, it can be seen that UO_2^{2+} was the dominant species at low pH, which suggested that the amidoxime group can function as a bidentate ligand for the uranyl cation[13, 16]. The lone pairs of electrons on the amino nitrogen and the oxime oxygen combined with the positive UO_2^{2+} and formed a five-membered ring with U(VI)[14]. The oxime oxygen can be deprotonated with the assistance of metal ion:

$$R-C(NH_2)N-OH \leftrightarrow R-C(NH_2)N-O^- + H^+ \quad (16)$$

$$2R-C(NH_2)N-O^- + UO_2^{2+} \leftrightarrow UO_2(R-C(NH_2)N-O)_2 \quad (17)$$

As previous studies showed, when pH was lower than 2, the main form of uranium in solution was UO_2^{2+} ions, and they had lower competition than the protons for the banding sites on the biosorbent [33-34]. As pH increased, the amount of H^+ ions from the chelation reactions decreased, the deprotonation of the functional groups reduced the repulsion between AMAN and UO_2^{2+}, and the adsorption efficiency increased. However, when pH value was greater than 7, the adsorbed amount of U(VI) ions decreased with increasing pH, which might be attributed to the hydrolysis of U(VI) leading to noncomplexible species such as $UO_2(OH)_3^-$ and $UO_3(OH)_7^-$, and the repulsion between these anions and the negatively

charged surface of AMAN was enhanced at high pH[16].Therefore, the subsequent experiments were carried out with the initial pH 5 and 7 for RAN and the AMAN, respectively.

4.3 Effect of contact time

Fig.6 shows the effect of contact time on the adsorption of U(VI) by RAN and AMAN. As can be seen from the figure, the biosorption capacity of AMAN was much higher than that of RAN all the time, and this indicates that the amidoxime modification could significantly improve the adsorption performance of RAN for U(VI). The capacities of RAN and AMAN at equilibrium were achieved in 120 min and 180 min, respectively, which were selected as the contact time in the subsequent studies. It can be inferred that the adsorption capacity during the early phase may depend on the strong chelation of amidoxime functional groups with U(VI) and the electrostatic interactions[37], and the adsorption capacity during the late phase may be dependable on the complexation, micro-precipitation, inner diffusion and saturation of the binding sites.

4.4 Effect of initial U(VI) concentration

The effect of the initial U(VI) concentration on the adsorption was investigated, and the results are shown in Fig.7， which shows that the adsorption capacity of RAN and AMAN increased from 0.79 to 2.93 mg/g and from 0.99 to 3.86 mg/g, respectively, as the initial uranium

concentration increased from 0.2 mg/L to 0.8 mg/L. It should be noted that the adsorption capacity for U(VI) did not reach saturation. By comparing Fig.7(a) with Fig.7(b), it can be found that the biosorption capacity of the AMAN for U(VI) was higher than that of RAN at the same initial concentration of U(VI), demonstrating that the AMAN was a highly efficient biosorbent for adsorption of uranium.

The maximum value of adsorption distribution constant (K_d) shows the characteristic of the adsorbent, and the greater it is, the better the adsorbent is. It can be seen from Fig.7 that the adsorption distribution constants of RAN and AMAN were 587885 and 12648160 mL/g at initial uranium concentration of 0.2 and 0.5 mg/L, respectively. This also shows that the adsorption performance of AMAN of U(VI) from low concentration radioactive wastewater was better than RAN. Therefore, the initial uranium concentration had great effect on the U(VI) extraction capacity, and the reason for this was probably that the initial uranium concentration provided a significant driving force to overcome the mass transfer resistance of uranium between adsorbent and solution [38, 39].

4.5 Effect of biosorbent dose

The effect of biosorbent dose on the removal efficiency is shown in Fig.8. It is observed that the removal efficiencies of U(VI) by RAN and AMAM increased with their dose, which may be attributed to the increase of the numbers of available biosorption sites [19]. For AMAN, the

removal efficiency increased from 87.06% to 98.85% when the biosorbent dose increased from 0.05 to 0.20 g/L. However, when the biosorbent dose further increased to 0.35 g/L, the removal efficiency gradually decreased to 91.15%. The reason for this may be that the electrostatic interactions between biosorbent particles can result in their agglomeration and decrease the number of available binding sites [40]. It can also be observed that the optimum doses of RAN and AMAN were both 0.20 g/L, but the maximum removal efficiency of the latter was actually higher than that of the former which was only 78.75%.

4.6 Adsorption isotherms

Equilibrium isotherm studies for the adsorption of U(VI) by RAN and AMAN were conducted with two parameter isotherm models, viz., Langmuir, Freundlich, and Dubinin-Radushkevich (D-R), and the results are shown in Fig.9(a), Fig.9(b) and Fig.9(c), respectively. The parameters obtained from the slopes and longitudinal coordinate intercepts of the linear plots of $1/q_e$ versus $1/C_e$, $\ln q_e$ versus $\ln C_e$, and $\ln q_e$ versus ε^2 were listed in Table 1. The Langmuir isotherm models of RAN and AMAN fitted better to the equilibrium data since their R^2 values were 0.968 and 0.994, respectively, which were higher than those of other models, indicating that the surface of the biosorbents was homogenous. Determination of the maximum uranium adsorption capacity of AMAN calculated from the Langmuir equation was 621 mg/g which was much

higher than that of RAN (4.314 mg/g) and the other materials listed in Table 2. AMAN with such a high sorption capability of U(VI) shows a potential of real applications in removal and recovery of U(VI) from large volumes of aqueous solutions.

Based on the values of R_L and 1/n which were less than 1, respectively, it could be seen that the adsorption process was feasible and favorable.

4.7 Kinetic modeling

The kinetic studies on the biosorption of U(VI) was conducted with pseudo first order, pseudo second order and intraparticle difussion models. The kinetic parameters k_1, k_2 and k_{id} for the models were calculated from the linear plots of $\log(q_{e1}-q_t)$ versus t (Fig.10a), t/q versus t (Fig.10b) and q_t versus $t^{1/2}$ (Fig.10c), respectively, and the results are shown in Table 3. It is clear that the pseudo-second-order model best described the adsorption process since the correlation coefficients of the pseudo second order models of the two biosorbents were over 0.999, while the correlation coefficients of the pseudo-first-order models of the two biosorbents were only 0.903 and 0.987, respectively, and those of the intraparticle difussion models were 0.8277 and 0.9782, respectively. Moreover, the q_e values for RAN and AMAN calculated from the pseudo-second-order model were 1.98 mg/g and 2.46 mg/g, respectively, which were more similar to the experimental results (2.04 mg/g, 2.47 mg/g). These results further indicate that the biosorption mechanism of

U(VI) by AMAN was mainly dominated by strong chemical sorption or surface complexation rather than mass transport [16,43].

As can be seen from Fig.10c, the data for AMAN fitted the intraparticle diffusion model, and the biosorption process of AMAN consisted of the initial steep-sloped portion from 0 to 180 min, which may be due to the external mass transfer, and a gentle-sloped portion from 180 to 720 min, which may be attributed to the intraparticle or pore diffusion. Based on these results, it can be concluded that the intraparticle diffusion was not the only rate-limiting step for U(VI) biosorption [44]. It can also be found by comparing the values of q_e for the two biosorbents that AMAN had greater boundary effect than RAN [45].

4.8 Thermodynamic studies

The influence of temperature on the process of U(VI) biosorption was investigated with Eq.(13) and Eq.(14) at the optimum pH and contact time. The enthalpy (ΔH^0) and entropy (ΔS^0) changes for the biosorption of U(VI) by RAN and AMAN were determined from the slope and the intercept of the line of $\ln K_d$ versus 1/T (Fig.11), respectively. The obtained thermodynamic parameters were presented in Table 4. The negative value of Gibbs free energy change (ΔG^0) indicates that the biosorption process was feasible and spontaneous [46]. Furthermore, the magnitude of ΔG^0 gradually increased with the rising temperature from 283 K to 303 K for both of the biosorbents, implying that the higher the

temperature was, the more efficient the biosorption process was. In addition, the positive values of ΔH^0 and ΔS^0 suggested the endothermic nature of U(VI) biosorption and the increase in randomness at the solid-solution interface during U(VI) uptake[47], respectively.

4.9 Selective adsorption of U(VI) by AMAN

The selective adsorption of U(VI) by AMAN was studied in the simulated water sample containing Ca, Mg, Pb, Fe, Co, etc.. The main initial mental ion concentrations were shown in Table 5, and the residual ion concentrations were detected by WYX-420 atomic absorption spectrophotometer. The metal ion distribution coefficient (D) and the selective adsorption coefficient (K) were calculated using Eq. (18) and Eq. (19), respectively:

$$D=\frac{(c_0-c_e)\ v}{c_e W} \quad (18)$$

$$K_{U(VI)/M}=\frac{D_{U(VI)}}{D_M} \quad (19)$$

where V and W are the solution volume (L) and the adsorbent dose (g), respectively.

Table 5 shows that although the concentrations of other metal ions were obviously higher than that of U(VI), the D values of other metal ions were much lower than that of U(VI) and $K_{U(VI)/M}$ values of other metal ions were much higher than that of U(VI). This indicates that Ca, Mg, Pb, Fe, Co had no obvious interference with the adsorption of U(VI) by

AMAN, the amidoxime functionalization in this study was effective, and AMAN had desirable selectivity for U(VI) ions in solution containing other metal ions.

4.10 Desorption, regeneration and reuse studies

An adsorbent for the practical application in water treatment should have both excellent selectivity and good desorption-regeneration-reuse property[48]. In this paper, HCl, HNO_3, NaOH, Na_2CO_3, $NaHCO_3$ and EDTA-NA, each in concentration of 0.1 mol/L, were used to conduct experiments on the desorption, and the results are given in Table 6. It can be seen that 0.1 mol/L HCl was the best eluant for the desorption, and the desorption rate of U(VI) amounted to 94.67%. Experiments on 8 cycles of adsorption-desorption of AMAN were conducted using 0.1 mol/L HCl, and the results are presented in Fig.12, which shows that the desorption rate was 87.28% at the 8th cycle of consecutive adsorption-desorption. During the adsorption-desorption processes, only a little loss of biosorption capacity happened, indicating that AMAN had good biosorption capacity and recycling biosorption capability.

5 Conclusions

In this study, a novel material AMAN was prepared, the adsorption of U(VI) from radioactive wastewater in U(VI) concentration of less than 1 mg/L by AMAN and RAN were investigated. The maximum adsorption efficiency of U(VI) from the low concentration radioactive wastewater

with concentration of 0.5 mg/L by AMAN amounted to 98.85% under the optimum adsorption conditions, the adsorption equilibrium data best fitted to Langmuir isotherm model, and its maximum biosorption capacity for U(VI) was estimated to be 621 mg/g at 298 K. The kinetics for biosorption of U(VI) by AMAN was found to be in good agreement with pseudo-second-order model, and the biosorption process was spontaneous, feasible and endothermic. The SEM-EDS study indicates that much more UO_2^{2+} ions attached onto AMAN than onto RAN. The FT-IR study shows that the $-NH_2$ and =N-OH groups of amidoxime were the dominated ones for binding UO_2^{2+} ions. The selective adsorption experiment indicates that AMAN had excellent selective adsorption capability in the existence of other metal ions since the amidoxime on it could chelate with U(VI) ions and form stable five-membered complexes. 0.1 M HCl was the most effective desorption agent, and the desorption rate amounted to as high as 87.28% after 8 cycles of adsorption and desorption. The convenient and fast easy operation and high selective sorption performance indicate that AMAN could be potentially used as a highly effective material for the removal and recovery of U(VI) from contaminated wastewater and seawater.

Acknowledgements

This research was supported by the National Natural Science Foundation of China (U1401231,91326106,11405081), the Development

Program for Science and Technology for National Defense (B3720132001), and the Construction Program for the Key Disciplines in Hunan Province.

References

[1] S.K. Yang, N. Tan, X.M. Yan, F. Chen, W. Long, Y.C. Lin, Thorium(IV) removal from aqueous medium by citric acid treated mangrove endophytic fungus Fusarium sp. #ZZF51, Marine Pollution Bulletin. 74 (2013) 213-219.

[2] K.K. Kumar, M.K. Prasad, B. Sarada, Studies on biosorption of nickel using immobilized fungus, rhizomucor tauricus, BioResources. 7 (2012) 5059-5073.

[3] I.W. Mwangi, J.C. Ngila. Removal of heavy metals from contaminated water using ethylenediamine-modified green seaweed (Caulerpa serrulata), Physics and Chemistry of the Earth. 50-52 (2012) 111-120.

[4] Y.N. Mata, M.L. Blázquez, A. Ballester, Biosorption of cadmium, lead and copper with calcium alginate xerogels and immobilized Fucus vesiculosus, Journal of Hazardous Materials. 163 (2009) 555-562.

[5] J.X Li, Z.Q. Guo, S.W. Zhang and X.K Wang. Enrich and seal radionuclides in magnetic agarose microspheres, Chemical Engineering Journal. 172 (2011) 892-897.

[6] V. Farkas, A. Felinger, A. Hegedusova, Comparative study of the kinetics and equilibrium of phenol biosorption on immobilized white-rot fungus Phanerochaete chrysosporium from aqueous solution, Colloids and Surfaces B: Biointerfaces. 103 (2013) 381-390.

[7] M. Ghasemi, A.R. Keshtkar, R. Dabbagh, Biosorption of uranium (VI) from aqueous solutions by Ca-pretreated Cystoseira indica alga: Breakthrough curves studies and modeling, Journal of Hazardous Materials. 189 (2011) 141-149.

[8] A. Bingol, A. Aslan, A. Cakici, Biosorption of chromate anions from aqueous solution by a cationic surfactant-modified lichen (Cladonia rangiformis (L.)), Journal of Hazardous Materials. 161 (2009) 747-752.

[9] T.S. Anirudhan, L. Divya, P.S. Suchithra, Kinetic and equilibrium characterization of uranium(VI) adsorption onto carboxylate-functionalized poly (hydroxyethylmethacrylate)-grafted lignocellulosics, Journal of Environmental Management. 90 (2009) 549-560.

[10] M.H. Song, S.W. Won, Y.S. Yun, Decarboxylated polyethylenimine-modified bacterial biosorbent for Rubiosorption from Ru-bearing acetic acid wastewater, Chemical Engineering Journal. 230 (2013) 303-307.

[11]S.W Zhang, M.Y. Zeng, W.Q. Xu, J.X Li, J. Li, J.Z. Xu and X.K Wang. Polyaniline nanorods dotted on graphene oxide nanosheets as a novel super adsorbent for Cr(VI), Dalton Transactions.(2013) DOI: 10.1039/c3dt50149c.

[12] D.X. Ding, X. Tan, N. Hu, Removal and recovery of uranium (VI) from aqueous solutions by immobilized Aspergillus niger powder beads, Bioprocess and Biosystems Engineering. 35 (2012) 1567-1576.

[13] Y.G Zhao, J.X. Li, S.W. Zhang and X.K Wang. Amidoxime-functionalized magnetic mesoporous silica for selective sorption of U(VI), RSC Advances. 4(2014)32710-32717.

[14] D.D. Shao, J.X. Li and X.K Wang. Poly(amidoxime)-reduced graphene oxide composites as adsorbents for the enrichmentof uranium from seawater, Science china chemistry. 57(2014):1449-1458.

[15] F.L. Huang, Y.F. Xu, S.Q. Liao, Preparation of Amidoxime Polyacrylonitrile Chelating Nanofibers and Their Application for Adsorption of Metal Ions, Materials. 6 (2013) 969-980.

[16] Y.G Zhao, J.X Li, L.P Zhao, S.W Zhang, Y.S Huang, X.L Wu and X.K Wang. Synthesis of amidoxime-functionalized Fe_3O_4@SiO_2 core–shell magnetic

microspheres for highly efficient sorption of U(VI). Chemical Engineering Journal. 235 (2014) 275-283.

[17] A.S. Saini, J.S. Melo, Biosorption of uranium by melanin: Kinetic, equilibrium and thermodynamic studies, Bioresource Technology. 149 (2013) 155-162.

[18] A. Cecal, D. Humelnicu, V. Rudic, Uptake of uranyl ions from uranium ores and sludges by means of Spirulina platensis,Porphyridium cruentum and Nostok linckia alga, Bioresource Technology. 118 (2012) 19-23.

[19] U.A. Guler, M. Sarioglu, Single and binary biosorption of Cu(II), Ni(II) and methylene blue by raw and pretreated Spirogyra sp: Equilibrium and kinetic modeling, Journal of Environmental Chemical Engineering, 1 (2013) 369-377.

[20] C. Gok, S. Aytas, Biosorption of uranium(VI) from aqueous solution using calcium alginate beads, Journal of Hazardous Materials. 168 (2009) 369-375.

[21] S. Tunali, T. Akar, A.S. Ozcan, Equilibrium and kinetics of biosorption of lead(II) from aqueous solutions by Cephalosporium aphidicola, Separation and Purification Technology. 47 (2006) 105-112.

[22] B. Nagy, A. Maicaneanu, C. Indolean, Comparative study of Cd(II) biosorption on cultivated Agaricus bisporus and wild Lactarius piperatus based biocomposites. Linear and nonlinear equilibrium modelling and kinetics, Journal of the Taiwan Institute of Chemical Engineers. 45 (2013) 921-929.

[23] F.T. Chi, S. Hu, J. Xiong, Adsorption behavior of uranium on polyvinyl alcohol-g-amidoxime: Physicochemical properties, kinetic and thermodynamic aspects, Science china chemistry. 56 (2013) 1495-1503.

[24] A.L. John-Peter, T. Viraraghavan, Removal of thallium from aqueous solutions by modified spergillus niger biomass, Bioresource Technology. 99 (2008) 618-625.

[25]Y. Khambhaty, K. Mody, S. Basha, B. Jha. Kinetics, equilibrium and thermodynamic studies on biosorption of hexavalent hromium by dead fungal

biomass of marine Aspergillus niger, Chemical Engineering Journal. 145 (2009) 489-495.

[26] S. Kushwaha, P. Padmaja, Sudhakar. Sorption of uranium from aqueous solutions using palm-shell-based adsorbents: a kinetic and equilibrium study, Journal of Environmental Radioactivity. 126 (2013) 115-124.

[27] S.P. Chen, J.X. Hong, H.X. Yang, Adsorption of uranium (VI) from aqueous solution using a novel graphene oxide-activated carbon felt composite, Journal of Environmental Radioactivity. 126 (2013) 253-258.

[28] O. Genc, Y. Yalcınkaya, E. Buyuktuncel, Uranium recovery by immobilized and dried powdered biomass: characterization and comparison, International journal of mineral processing. 68 (2003) 93-107.

[29] M.R. Lutfor, S. Silong, W.M.Z.W. Yunus, Polymer Bearing Amidoxime Groups for Extraction of Arsenic From Aqueous Media, Journal of Applied Polymer Science. 76(2000)516-523.

[30] K. Saeed, S. Haider, T.J. Oh, Preparation of amidoxime-modified polyacrylonitrile (PAN-oxime) nanofibers and their applications to metal ions adsorption, Journal of Membrane Science. 322 (2008) 400-405.

[31] S.S. Basarır, N.P. Bayramgil. The uranium recovery from aqueous solutions using amidoxime modified cellulose derivatives. IV. Recovery of uranium by amidoximated hydroxypropyl methylcellulose, Cellulose. 20 (2013) 827-839.

[32] J.X. Yu, M. Tong, X.M. Sun, Cystine-modified biomass for Cd(II) and Pb(II) biosorption, Journal of Hazardous Materials. 143 (2007) 277-284.

[33] G.M. Maciel, C.G.M. Souza, C.A.V. Araújo, E. Bona, C.W.I.Haminiuk, R. Castoldi, A. Bracht，R. Marina. Biosorption of herbicide picloram from aqueous solutions by live and heat-treated biomasses of Ganoderma lucidum (Curtis) P. Karst and Trametes sp., Chemical Engineering Journal. 215-216 (2013) 331-338.

[34] S.P. Chen, J.X. Hong, H.X. Yang, Adsorption of uranium (VI) from aqueous solution using a novel graphene oxide-activated carbon felt composite, Journal of Environmental Radioactivity. 126 (2013) 253-258.

[35] S. Aytas, D.A. Turkozu, C. Gok, Biosorption of uranium(VI) by bi-functionalized low cost biocomposite adsorbent, Desalination. 280 (2011) 354-362.

[36] S. Akyil, M.A.A. Aslani, M. Eral. Sorption characteristics of uranium onto composite ion exchangers, Journal of Radioanalytical and Nuclear Chemistry. 256 (2003) 45-51.

[37] S.V. Bhat, J.S. Melo, B.B. Chaugule. Biosorption characteristics of uranium(VI) from aqueous medium onto Catenella repens, a red alga, Journal of Hazardous Materials. 158 (2008) 628-635.

[38] C. Pang, Y.H. Liu, X.H. Cao, M. Li, G.L. Huang, R. Hua. Biosorption of uranium(VI) from aqueous solution by dead fungal biomass of Penicillium citrinum. Chemical Engineering Journal. 170 (2011) 1-6.

[39] J. Bai, H.J. Yao, F.L. Fan, M.S. Lin, L.N. Zhao, H.J. Ding, F.A. Lei. Biosorption of uranium by chemically modified Rhodotorula glutinis. Journal of Environmental Radioactivity. 101 (2010) 969-973.

[40] Y.G Zhao, J.X Li, S.W Zhang, H. Chen and D.D. Shao. Efficient enrichment of uranium(VI) on amidoximated magnetite/graphene oxide composites, RSC Advances. 3(2013)18952-18959.

[41] L.Y. Yuan, Y.L. Liu,W.Q. Shi, Z.J. Li, J.H. Lan,Y.X. Feng,Y.L. Zhao,Y.L. Yuan, Z.F. Chai. A novel mesoporous material for uranium extraction, dihydroimidazole functionalized SBA-15. Journal of Materials Chemistry. 22(2012)17-19.

[42] C. Pang, Y.H. Liu, X.H. Cao, R. Hua. C.X. Wang. C.Q. Li. Adsorptive removal of uranium from aqueous solution using chitosan-coated attapulgite. J Radioanal Nucl Chem. 286 (2010)185-193.

[43] Y.S. Huang, J.X. Li, X.P. Chen and X.K Wang. Applications of conjugated polymer based composites in wastewater purification, RSC Advances.4(2014)62160-62178.

[44] A.R. Khataee, F. Vafaei, M. Jannatkhah. Biosorption of three textile dyes from contaminated water by filamentous green algal Spirogyra sp.: Kinetic, isotherm and thermodynamic studies, International Biodeterioration & Biodegradation. 83 (2013) 33-40.

[45] C. Gok, S. Aytas. Biosorption of uranium(VI) from aqueous solution using calcium alginate beads, Journal of Hazardous Materials. 168 (2009) 369-375.

[46] A.Y. Dursun. A comparative study on determination of the equilibrium, kinetic and thermodynamic parameters of biosorption of copper(II) and lead(II) ions onto pretreated Aspergillus niger, Biochemical Engineering Journal. 28 (2006) 187-195.

[47] L. Li, D.X. Ding, N. Hu, P.K. Fu, X. Xin, Y.D. Wang. Adsorption of U(VI) ions from low concentration uranium solution by thermally activated sodium feldspar, Journal of Radioanalytical and Nuclear Chemistry. 299 (2014) 681-690.

[48] D.D Shao, G.S Hou, J.X Li, T. Wen, X.M. Ren and X.K Wang. PANI/GO as a super adsorbent for the selective adsorption of uranium(VI), Chemical Engineering Journal. 255 (2014) 604-612.

Figure captions

Fig.1. Synthesis of AMAN: (a) reaction between the KH-570 modified RAN and Polyacrylonitrile (PAN); (b) oximation reaction.

Fig.2. FT-IR spectra of (a) RAN, (b) KH-570 modified RAN, (c) grafting of polyacrylonitrile to KH-570- RAN, (d) AMAN, and (e) AMAN after adsorption of U(VI).

Fig.3. SEM images of (a) RAN, (b) AMAN before adsorption of U(VI), and (c) AMAN after adsorption of U(VI).

Fig.4. SEM-EDX images of AMAN after adsorption of U(VI).

Fig.5. Effect of initial pH on biosorption of U(VI) by RAN and AMAN. (for RAN: t=120 min, $C_{U(VI)\ initial}$=0.5mg/L, m/V=0.02 g/L, T=298 K; for AMAN: t=180 min, $C_{U(VI)\ initial}$=0.5mg/L, m/V=0.02 g/L, T=298 K).

Fig.6. Effect of contact time on biosorption of U(VI) by RAN and AMAN. (for RAN: pH=7, $C_{U(VI)\ initial}$=0.5mg/L, m/V=0.02 g/L, T=298 K; for AMAN: pH=5, $C_{U(VI)\ initial}$=0.5mg/L, m/V=0.02 g/L, T=298 K).

Fig.7. Effect of initial U(VI) concentration on the biosorption of U (VI) by RAN and AMAN (for RAN: pH=7, t=120 min, m/V=0.02 g/L, T=298 K; for AMAN: pH=5, t=180 min, m/V=0.02 g/L, T=298 K).

Fig.8. Effect of the biosorbent dose on the biosorption of U (VI) by RAN and AMAN (for RAN: pH=7, t=120 min, $C_{U(VI)\ initial}$=0.5mg/L , T=298 K; for AMAN: pH=5, t=180 min, $C_{U(VI)\ initial}$=0.5mg/L, T=298 K).

Fig.9. Plots of (a) Langmuir, (b) Freundlich, and (c) Dubinin-Radushkevich models for biosorption of U(VI) by RAN and AMAN(for RAN: pH=7, t=120 min, $C_{U(VI)\ initial}$=0.5mg/L; for AMAN: pH=5, t=180 min, $C_{U(VI)\ initial}$=0.5mg/L).

Fig.10. Plots of (a) pseudo-first-order, (b) pseudo-second-order, and (c) intraparticle diffusion models for biosorption of U(VI) by RAN and AMAN(for RAN: pH=7, $C_{U(VI)\ initial}$=0.5mg/L , T=298 K; for AMAN: pH=5, $C_{U(VI)\ initial}$=0.5mg/L, T=298 K).

Fig.11. Liner plot of $\ln K_d$ against 1/T for biosorption of U(VI) by RAN and AMAN(for RAN: pH=7, t=120 min, $C_{U(VI)\ initial}$=0.5mg/L; for AMAN: pH=5, t=180

min, $C_{U(VI)\ initial}$=0.5mg/L).

Fig.12. Desorption results for 5 cycles of biosorption-desorption of U(VI) by and from AMAN(pH=5, t=180 min, $C_{U(VI)\ initial}$=0.5mg/L, m/V=0.02 g/L, T=298 K).

Figures

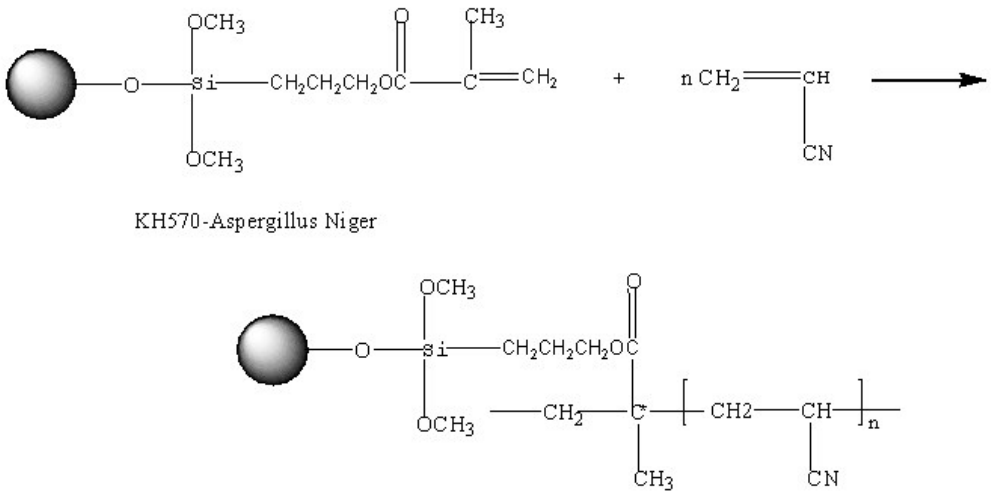

Fig.1.

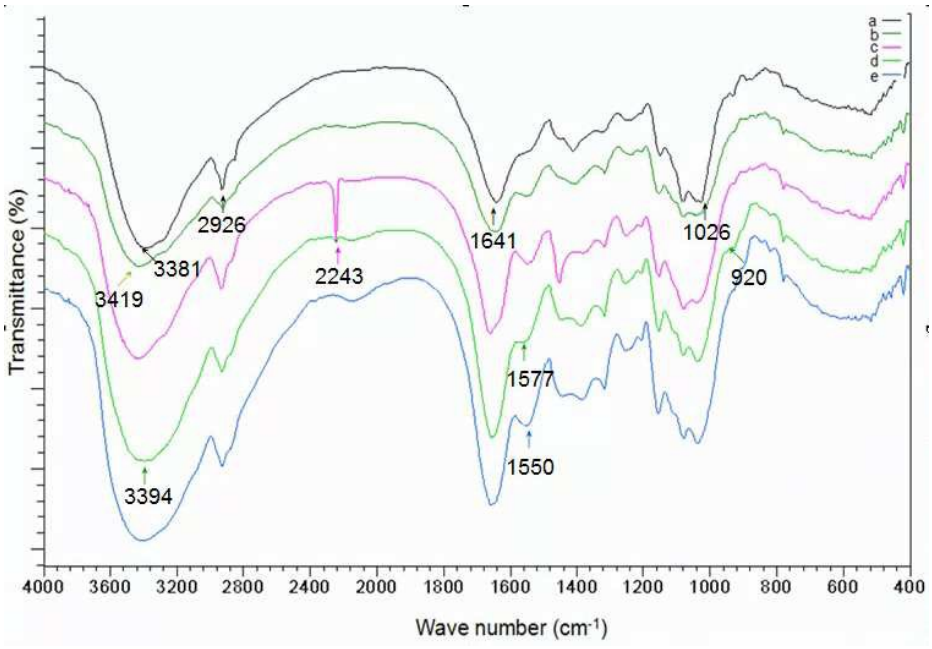

Fig.2.

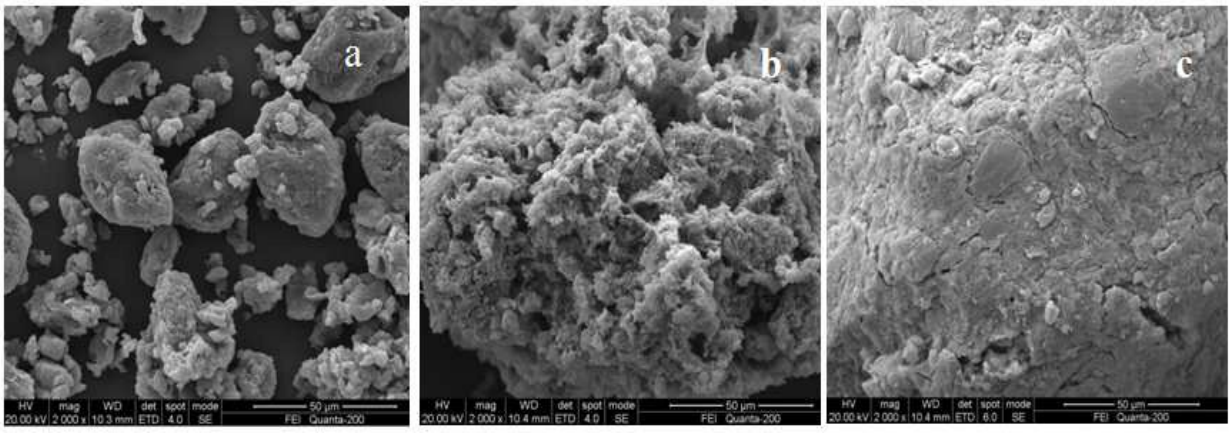

Fig.3.

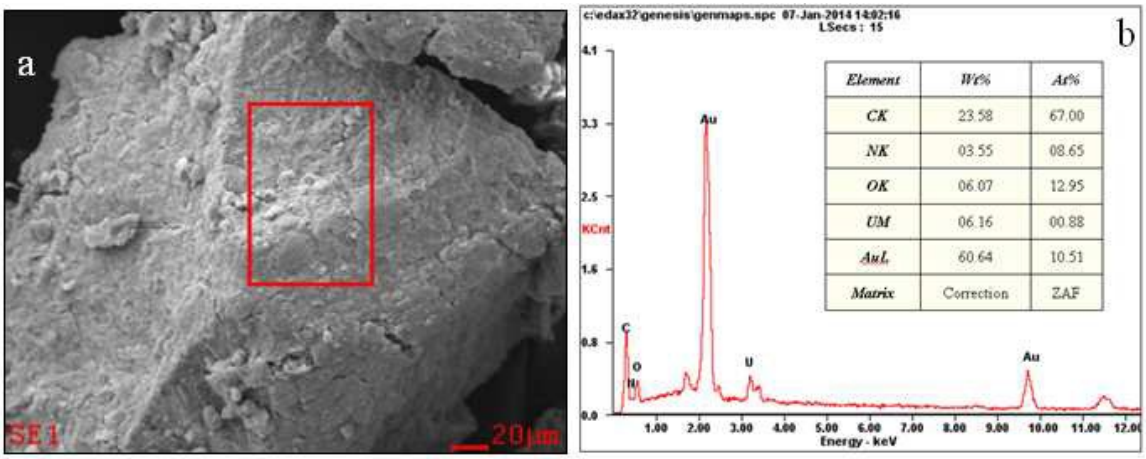

Fig.4.

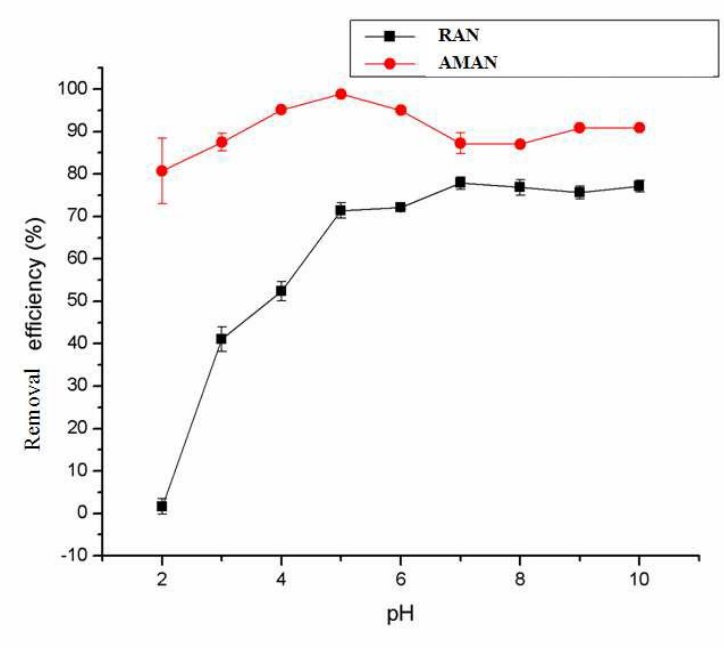

Fig.5.

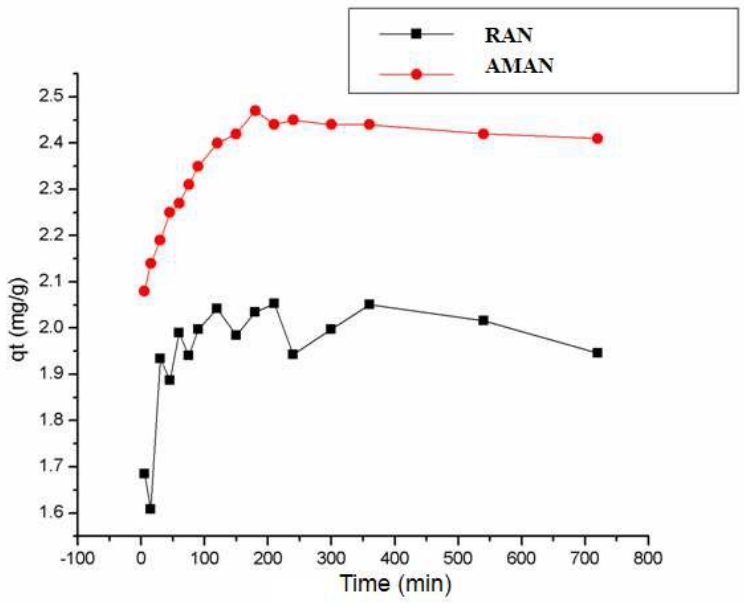

Fig.6.

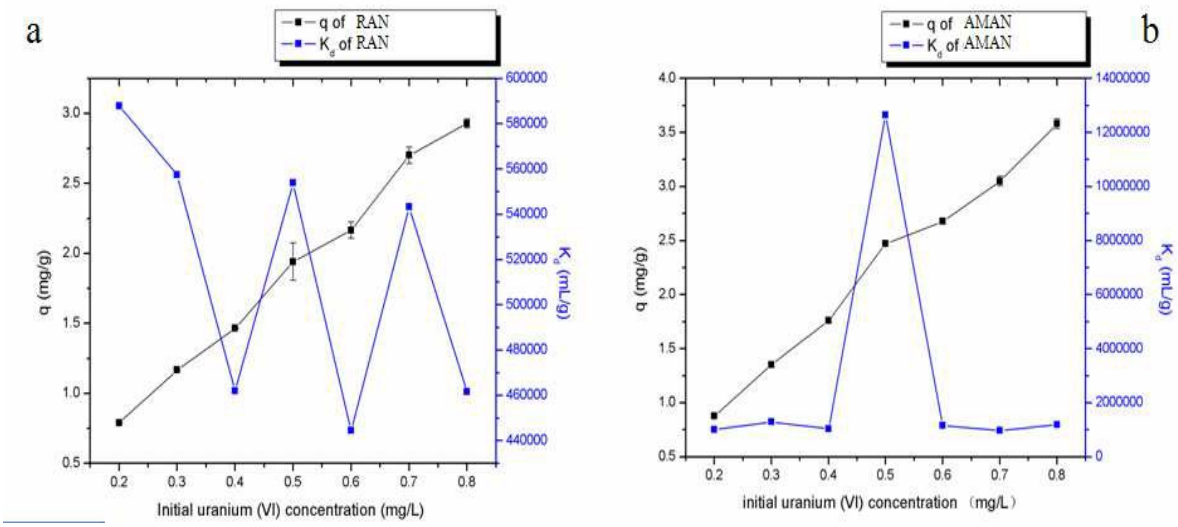

Fig.7.

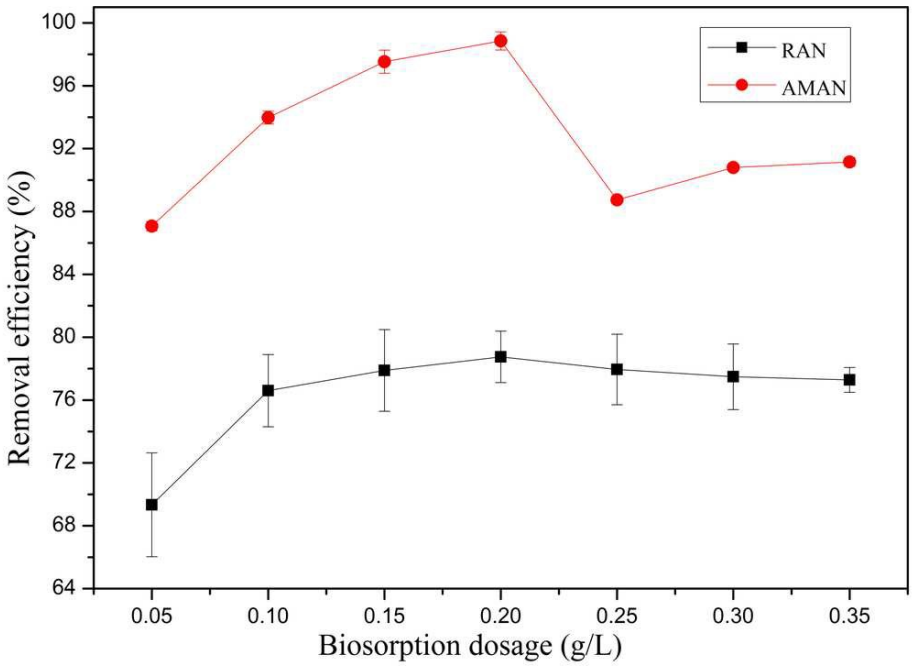

Fig.8.

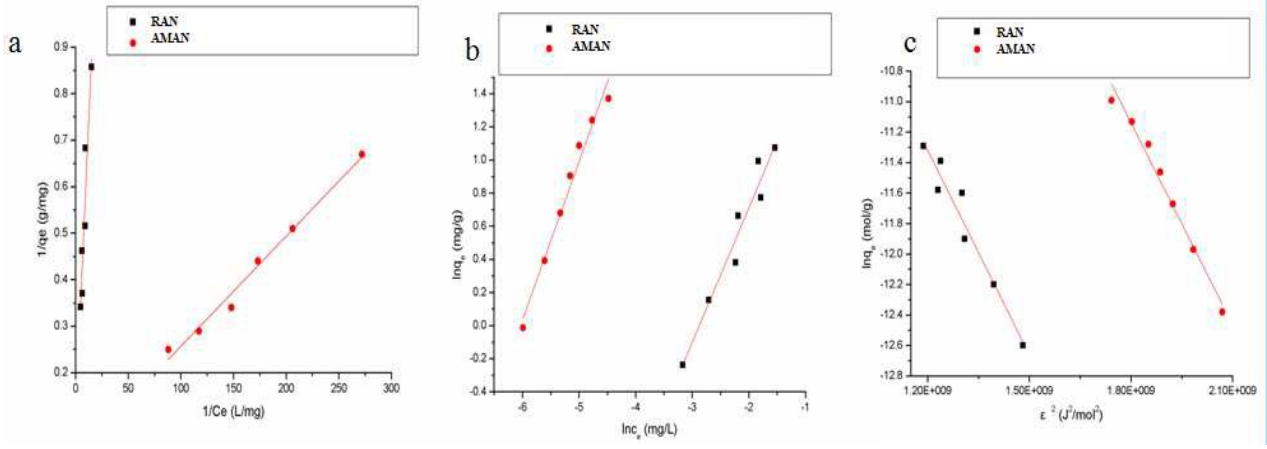

Fig.9.

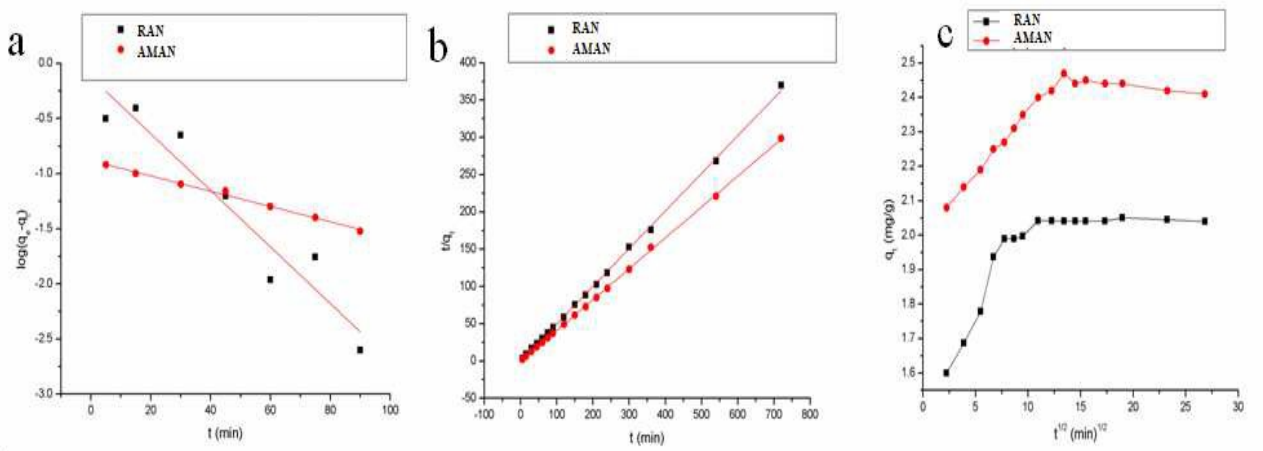

Fig.10.

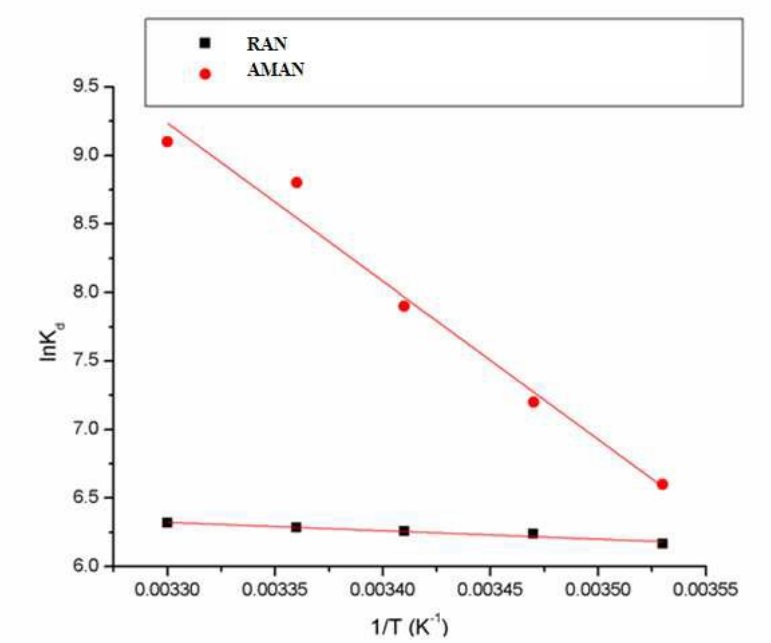

Fig.11.

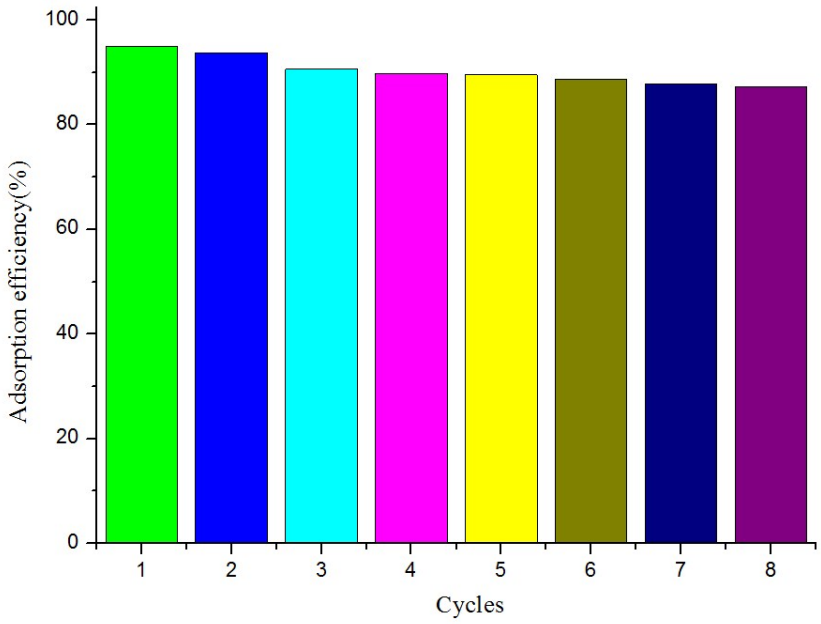

Fig.12.

Tables

Table 1. Langmuir, Freundlich and Dubinin-Radushkevich constants calculated using linear regression analysis for the biosorption of U(VI) by RAN and AMAN

Bio-sorbent	Langmuir				Freundlich			Dubinin-Radushkevich			
	q_{max} (mg/g)	b (L/mg)	R^2	R_L	K_F (L/g)	1/n	R^2	q_{D-R} (mg/g)	B $(mol/J)^2$	E (KJ/ mol)	R^2
RAN	4.314	6.368	0.968	<1	6.14	0.584	0.941	3.71	$2.21x10^{-8}$	4.756	0.962
AMAN	621.0	3.97	0.994	<1	320.88	0.9558	0.975	0.0418	$4.42x10^{-9}$	10.63	0.979

Table 2. Comparison of the U(VI) sorption capacity of AMAN with other sorbents

Sorbents	Experimental conditions	q_{max}(mg/L)	Reference
Catenella repens. a red alga	pH=4.5，T=303K，t=0.75h	303	37
Penicillium citrinum	pH=6，T=298K，t=5h	255.1	38
Rhodotorula glutinis	pH=6，T=298K，t=0.5h	187	39
Methanol-treated Rhodotorula glutinis	pH=6，T=298K，t=0.5h	350	39
Formaldehyde-treated Rhodotorula glutinis	pH=6，T=298K，t=0.5h	360	39
dihydroimidazole functionalized SBA-15	pH=5，T=298K，t=5h	268	41
The chitosan coated acid-treated attapulgite beads	pH=5.5，T=308K，t=4h	294.99	42
The chitosan coated natural attapulgite beads	pH=5.5，T=308K，t=4h	264.55	42
pure chitosan beads	pH=5.5，T=308K，t=4h	373.13	42
The amidoxime modified Aspergillus niger	pH=5, T=298 K, t=3h	621	this work

Table 3. Kinetic parameters for biosorption of U(VI) by RAN and AMAN

Bio-sorbent	Pseudo-first order			Pseudo-second order				Intraparticle diffusion			
	q_e (mg/g)	k_1 (min^{-1})	R^2	q_e (L/g)	k_2 (g/mg/min)	H (mg/g/min)	R^2	K_{id} (mg/g/$min^{0.5}$)	R^2	C (mg/g)	q_{e1} (mg/g)
RAN	0.749	0.059	0.903	1.98	-0.367	-1.449	0.9991	0.0517	0.8277	1.52	2
AMAN	0.131	0.016	0.991	2.46	-0.413	-2.5	0.9999	0.0119	0.9782	2.05	2.47

Table 4. Thermodynamic parameters for biosorption of U(VI) by RAN and AMAN.

Bio-sorbent	ΔH^0 (KJ/mol)	ΔS^0 (J/mol/K)	ΔG^0（KJ/mol）				
			283K	288K	293K	298K	303K
RAN	5.09	9.37	-14.51	-14.93	-15.25	-15.57	-15.91
AMAN	95.97	393.5	-15.53	-17.24	-19.24	-21.80	-22.92

Table 5. Selective adsorption of U(VI), Mg, Ca, Pb, Fe, Co by AMAN

	U (mg/L)	Mg (mg/L)	Ca (mg/L)	Pb (mg/L)	Fe (mg/L)	Co (mg/L)
Before adsorption	0.014	1503	513.9	0.569	0.435	0.333
After adsorption	0.009	1123	458.2	0.5	0.42	0.323
D	3.259	1.69	0.608	0.691	0.066	0.166
$K_{U(VI)/M}$	1	1.929	5.361	4.719	49.238	19.692

1 **Table 6.** Desorption rate for different desorption agents

Desorption agent	Desorption rate (%)
HCl	94.67
HNO_3	91.02
NaOH	88.97
EDTA-NA	46.85
Na_2CO_3	21.04
$NaHCO_3$	19.73

2
3
4